

## Specific Heat of the Ca-Intercalated Graphite Superconductor $\text{CaC}_6$

J. S. Kim,\* R. K. Kremer, and L. Boeri

*Max-Planck-Institut für Festkörperforschung, Heisenbergstraße 1, 70569 Stuttgart, Germany*

F. S. Razavi

*Department of Physics, Brock University, St. Catharines, Ontario L2S 3A1, Canada*

(Received 7 February 2006; published 2 June 2006)

The superconducting state of Ca-intercalated graphite  $\text{CaC}_6$  has been investigated by specific heat measurements. The characteristic anomaly at the superconducting transition ( $T_c = 11.4$  K) indicates clearly the bulk nature of the superconductivity. The temperature and magnetic field dependence of the electronic specific heat are consistent with a fully gapped superconducting order parameter. The estimated electron-phonon coupling constant is  $\lambda = 0.70 \pm 0.04$ , suggesting that the relatively high  $T_c$  of  $\text{CaC}_6$  can be explained within the intermediate coupling BCS approach.

DOI: [10.1103/PhysRevLett.96.217002](https://doi.org/10.1103/PhysRevLett.96.217002)

PACS numbers: 74.70.Ad, 74.25.Bt

The recent discovery of superconductivity in Ca- and Yb-intercalated graphite has refocused considerable interest onto graphite intercalated compounds (GICs) [1,2]. The superconducting transition temperature for Ca- and Yb-intercalated graphite is  $T_c \approx 11.5$  and 6.5 K, respectively, significantly higher than the alkali-metal intercalated graphite phases studied in the 1980s [3]. Similar to  $\text{MgB}_2$  where the hexagonal  $B$  sheets are intercalated with Mg, in the GICs the Ca or Yb atoms are sandwiched by the honeycomb graphene layers. The intercalated metal ions act as donors and transfer charge into the host graphene layers, resulting in partially filled graphene  $\pi$  bands. In contrast to  $\text{MgB}_2$  with a strong electron-phonon ( $e$ -ph) coupling of the  $B$   $\sigma$  bands, the coupling strength of the graphite  $\pi$  bands to in-plane phonon modes is expected to be small. Also out-of-plane phonon modes will not couple to the  $\pi$  band because of the antisymmetric character of the  $\pi$  orbitals. Thus the superconducting mechanism for the GICs could be rather different than that of  $\text{MgB}_2$ .

The superconducting mechanism, now under debate, relies on the other partially filled bands: the so-called interlayer bands. From a detailed comparison between the superconducting and nonsuperconducting GICs, Csányi *et al.* found that the filling of the interlayer state is essential for stabilizing the superconductivity in GICs [4]. Based on this result and considerations about the layered structure of the GICs, they proposed an unconventional electronic pairing mechanism involving excitons [5] or low-energy acoustic plasmons [6]. The latter has been discussed as a possible mechanism for the high  $T_c$  of the intercalated layered metal halide nitrides [7]. Soon after, however, Mazin [8] and Calandra and Mauri [9] suggested that the interlayer band originates from the  $s$  band of the intercalant, and an ordinary  $e$ -ph coupling mechanism involving the intercalant phonon and the out-of-plane  $C$  phonon modes would be sufficient to explain the relatively high  $T_c$  in the GICs. In order to shed light on this con-

trovery, further experimental studies on the superconducting properties of the GICs are required.

Specific heat ( $C_p$ ) measurements are known to be a powerful tool to investigate the superconducting states. Since  $C_p$  probes the quasiparticle excitations across the superconducting gap, its temperature and magnetic field dependence reflect the nature of the superconducting state such as gap symmetry, the presence of multigaps, and coupling strength between electrons and phonons (or other bosonic excitations). So far, there has been no  $C_p$  study on the superconducting state of the GICs, mostly because the low  $T_c$  was experimentally difficult to reach and the sample homogeneity was not sufficient for reliable studies. In this Letter, we report the temperature and magnetic field dependence of  $C_p$  for high-quality bulk  $\text{CaC}_6$  samples. In zero-field measurements we observe a sharp  $C_p$  anomaly at  $T_c \sim 11.4$  K. The detailed temperature and magnetic field dependence of  $C_p$  clearly show a fully gapped superconducting order parameter, and fit very well to the intermediate coupling BCS prediction.

The Ca-intercalated graphite samples were synthesized by reacting highly oriented pyrolytic graphite [Alfa Aesar, spread of the  $c$ -axis orientation  $0.4(1)^\circ$ ] with a molten lithium-calcium alloy at  $350^\circ$  for several weeks (cf. Ref. [2]). Since the metal alloy and the intercalated sample are air sensitive, all handling was done in purified argon atmospheres. X-ray diffraction patterns (not shown) dominantly show reflections of  $\text{CaC}_6$  (distance between graphene layers,  $d = 4.50$  Å), and contained no reflections related to nonintercalated graphite. Weak additional reflections [10] possibly due to Li/Ca-intercalated graphite phases [11] were observed. The contribution of the impurity phase is estimated to be less than 5% to the total heat capacity. The magnetic susceptibilities were determined in a SQUID magnetometer (Quantum Design). The superconducting transition temperature of our samples is  $T_c = 11.40(5)$  K (see the inset of Fig. 1), consistent with pre-

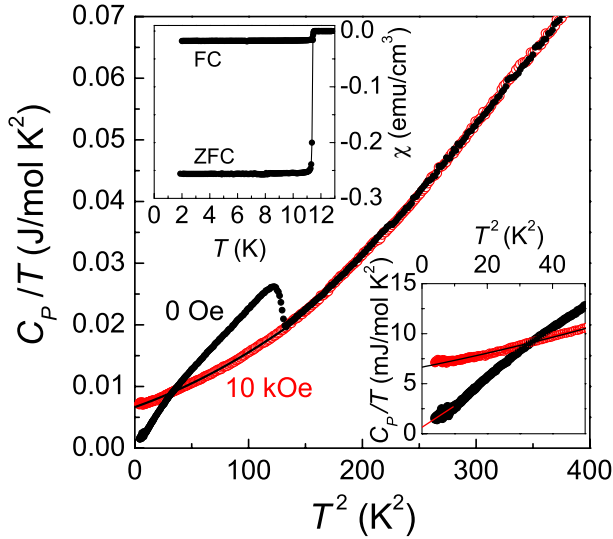


FIG. 1 (color online). Temperature dependence of the specific heat at  $H = 0$  and  $10$  kOe. The solid (black) line through the data points at  $H = 10$  kOe (also in the right inset) is a fit described in the text. Left inset: The temperature dependence of the susceptibility with  $H = 6$  Oe under zero-field-cooled (ZFC) and field-cooled (FC) modes. Right inset: The low temperature behavior of  $C_p(T)$ . The (red or gray) solid line for  $C_p(T)$  at  $H = 0$  is a linear fit for  $2 \text{ K} < T < 3 \text{ K}$ .

vious reports [2]. The transition width determined as the temperature difference between 10% and 90% diamagnetic shielding is only 0.1 K, smaller than found in previous reports [2]. After demagnetization correction, the volume fraction was estimated to be  $\approx 100\%$ . The heat capacity for a sample of  $\approx 5$  mg was measured using a PPMS calorimeter (Quantum Design) employing the relaxation method. To thermally anchor the crystals to the sapphire sample platform and to orient the samples with respect to the magnetic field ( $H \parallel c$ ), a minute amount of Apiezon  $N$  grease was used. The heat capacity of the platform and the grease, which amounted to  $\approx 40\%$ – $60\%$  over the whole temperature range, was determined in a separate run and subtracted from the measurements for the samples.

Figure 1 shows the temperature dependence of  $C_p$  at  $H = 0$  and  $H = 10$  kOe applied along the  $c$  axis. A sharp anomaly at  $T_c$  is resolved, indicating the bulk nature of the superconductivity in our sample. The onset of 11.40 K determined from the specific heat jump is consistent with the  $T_c$  obtained from the susceptibility measurements. A small offset of  $C_p/T$  at  $H = 0$  ( $\gamma_{\text{ns}} = 0.65 \pm 0.13 \text{ mJ/mol K}^2$ ) and a slight hump of  $C_p/T$  at  $H = 10$  kOe were observed below 3 K (see the right inset of Fig. 1), which probably originate from paramagnetic impurities or a nonsuperconducting fraction in our sample.  $\gamma_{\text{ns}}$  is only  $\sim 10\%$  of the Sommerfeld coefficient  $\gamma_N^*$  extracted from the normal state  $C_p(T)$  as discussed below. If we assume that  $\gamma_{\text{ns}}$  corresponds to the nonsuperconducting part of our sample, the volume fraction of the supercon-

ducting portion can be estimated as  $1 - (\gamma_{\text{ns}}/\gamma_N^*) \approx 90\%$ , proving a good quality of our GIC sample. The upper critical field  $H_{c2}^\perp$  along the  $c$  axis has been reported to be  $\sim 2.5$  kOe [2], thus the normal state  $C_p(T)$  can be obtained when the superconductivity is completely suppressed by a magnetic field  $H = 10$  kOe. A clear deviation from Debye  $T^3$  law seen in the normal state  $C_p$  has also been observed in the other alkali-metal GICs [12] and attributed to a contribution from the low-lying optical phonon modes. Recent *ab initio* calculations also show the presence of low frequency modes mainly involving vibration of the intercalated Ca [9,13]. The normal state  $C_p$  can be described by  $C_p = \gamma_N^* T + C_{\text{lattice}}(T)$  where  $\gamma_N^* T$  is the electronic contribution, and  $C_{\text{lattice}}(T) = \beta T^3 + \delta T^5$  is the lattice contribution. The solid line in Fig. 1 is the best fit to the  $H = 10$  kOe data below  $T < 12$  K, yielding the parameters  $\gamma_N^* = 6.66(1) \text{ mJ/mol K}^2$ ,  $\beta = 65.1(3) \mu\text{J/mol K}^4$ , and  $\delta = 0.256(3) \mu\text{J/mol K}^6$ . Considering the offset of  $C_p/T(H = 0)$ ,  $\gamma_{\text{ns}}$ , the Sommerfeld coefficient for the superconducting part of the sample is  $\gamma_N \approx \gamma_N^* - \gamma_{\text{ns}} = 6.01 \pm 0.14 \text{ mJ/mol K}^2$ . The corresponding Debye temperature  $\Theta_D(0)$  is 593(3) K, which is much higher than that of pure graphite [ $\Theta_D(0) = 413$  K] and the alkali-metal GICs (e.g., 235 K for  $\text{KC}_8$ ) [12], but comparable with  $\Theta_D(0) = 590$ – $710$  K for  $\text{LiC}_6$  [14].

The specific heat difference  $\Delta C_p$  between the normal and superconducting state is shown in Fig. 2. The solid line is the theoretical fit based on the “ $\alpha$  model” assuming an isotropic  $s$ -wave BCS gap  $\Delta(T)$  scaled by the adjustable parameter,  $\alpha = \Delta(0)/k_B T_c$  [15]. For the weak coupling limit,  $\alpha$  is 1.76. The detailed temperature dependence of

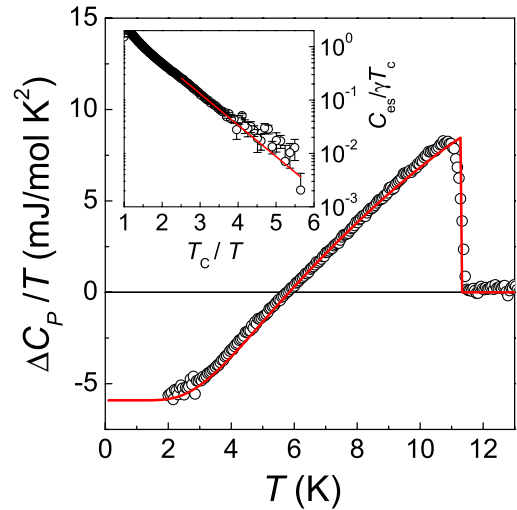


FIG. 2 (color online). Temperature dependence of  $\Delta C_p/T = C_p(H = 0)/T - C_p(H = 10 \text{ kOe})/T$ . The (red) solid line is the best fit according to the  $\alpha$  model assuming an isotropic  $s$ -wave BCS gap as described in the text. The electronic contribution of the specific heat  $C_{\text{es}}$  is plotted on a logarithmic scale against  $T_c/T$  in the inset. The (red) straight line in the inset is the exponential fit for  $2.5 < T_c/T < 5.5$ .

$\Delta C_P/T$  was fitted by three adjustable parameters:  $\alpha$ , the Sommerfeld coefficient  $\gamma$ , and  $T_c$ . The data are very well reproduced by  $\alpha = 1.776$ ,  $\gamma = 5.91$  mJ/molK<sup>2</sup>, and  $T_c = 11.30$  K. The normalized specific heat jump  $\Delta C_P/\gamma T_c$  is 1.432, which is close to the weak limit BCS value, 1.426. The normalized electronic specific heat  $C_{es}/\gamma T_c$  in the superconducting state is shown in the inset. The solid line is an exponential fit to the data for  $2.5 \leq T_c/T \leq 5.6$  using the form  $C_{es}/\gamma T_c \propto \exp(-0.82\alpha T_c/T)$  with  $\alpha = 1.65(1)$ .  $C_{es}$  exponentially vanishes for  $T \rightarrow 0$  K, clearly manifesting the absence of gap nodes in the superconducting order parameter. The  $\alpha$  value is somewhat lower than that from the  $\alpha$  model fit in which the ratio  $\Delta(0)/k_B T_c$  is mostly determined by the shape of the  $C_P$  jump near  $T_c$ . However, the discrepancy is less than 10%, in contrast to MgB<sub>2</sub> where the discrepancy is more than 60% due to the presence of two gaps [16].

Figure 3 shows the temperature dependence of  $C_P/T$  measured with different magnetic fields. Superconductivity is gradually suppressed, and the quasiparticle contribution increases with magnetic field.  $T_c(H)$  determined by the midpoint over the  $C_P$  anomaly is plotted in the inset with the error bar corresponding to the transition width.  $T_c(H)$  obtained from the susceptibility measurements (not shown) are in good agreement with those found from  $C_P(T)$ . For comparison, we also plot the predicted curve based on the Werthamer-Helfand-Hohenberg (WHH) theory [17].  $H_{c2}^\perp(T)$  shows a linear dependence down to  $T/T_c \approx 0.2$  and a clear deviation to the WHH prediction. Similar linear temperature dependence of  $H_{c2}$  has been

observed in other superconducting GICs such as KC<sub>8</sub> and KHgC<sub>4</sub> [18]. The best fit for low fields results in  $(dH_{c2}^\perp/dT)T_c = 219.1(8)$  Oe/K and the linear extrapolation of  $H_{c2}^\perp(T)$  to  $T = 0$  K yields  $H_{c2}^\perp(0) = 2.48$  kOe, which corresponds to the *ab*-plane coherence length,  $\xi_{ab}(0) \approx 360$  Å. From  $H_{c2}^\parallel(0) \approx 7$  kOe along the *ab* plane [2], the *c*-axis coherence length,  $\xi_c(0) \sim 130$  Å ( $\gg d = 4.50$  Å), is obtained. This result indicates the three-dimensional nature of superconductivity in CaC<sub>6</sub> [2].

The magnetic field dependence of the Sommerfeld coefficient  $\gamma(H)$  provides information about the superconducting gap symmetry. For a gapped superconductor, the quasiparticle excitations are expected to be confined in the vortex cores, and  $\gamma(H)$  is proportional to the density of vortices resulting in  $\gamma(H) \propto H$ . In contrast, when the superconducting gap is highly anisotropic or has a gap node, the delocalized quasiparticles near the gap minima cause a nonlinear magnetic field dependence such as  $\gamma(H) \propto H^{1/2}$  [19]. The normalized  $\gamma(H)$  for CaC<sub>6</sub> is displayed in Fig. 4.  $\gamma(H)$  for  $T \rightarrow 0$  K is determined from the linear fit for  $2 \text{ K} \leq T \leq 4 \text{ K}$  (see the inset of Fig. 4) after subtracting the offset of  $\gamma_{ns}(H=0)$ . As a consistency check, we also plot  $C_P(T, H)/T [\approx C_{es}(T, 0)/T + \gamma(T, H) + C_{lattice}/T]$  at the lowest temperature in the present measurements ( $T = 2$  K) after subtraction of  $C_P(H=0)/T [\approx C_{es}(T, 0)/T + C_{lattice}/T]$ . Both curves are normalized with  $\gamma(H = 10 \text{ kOe})$ .

As shown in Fig. 4,  $\gamma(H)$  increases linearly with  $H$  for low fields up to  $H \approx 0.3H_{c2}$ . This behavior is strongly

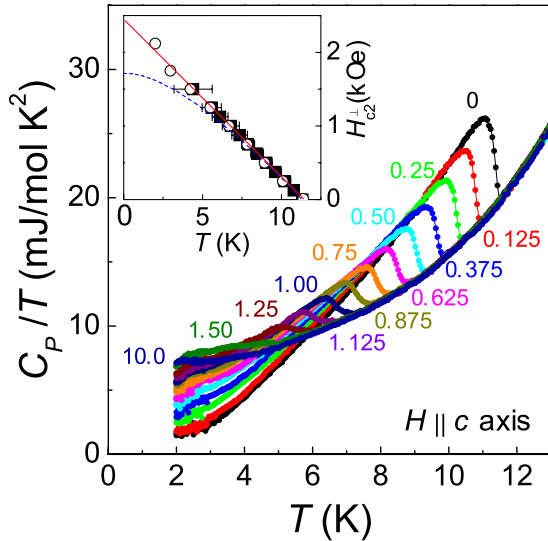


FIG. 3 (color online). Magnetic field dependence of the heat capacity for CaC<sub>6</sub>. The numbers next to the data correspond to the applied magnetic field (kOe) along the *c* axis. The inset shows the  $H_{c2}^\perp(T)$  for  $H \parallel c$  estimated from specific heat (■) and susceptibility (○). The (blue) dashed line demonstrates the WHH prediction [17], and the (red) solid line is a linear fit for the low magnetic field data ( $H \leq 1$  kOe).

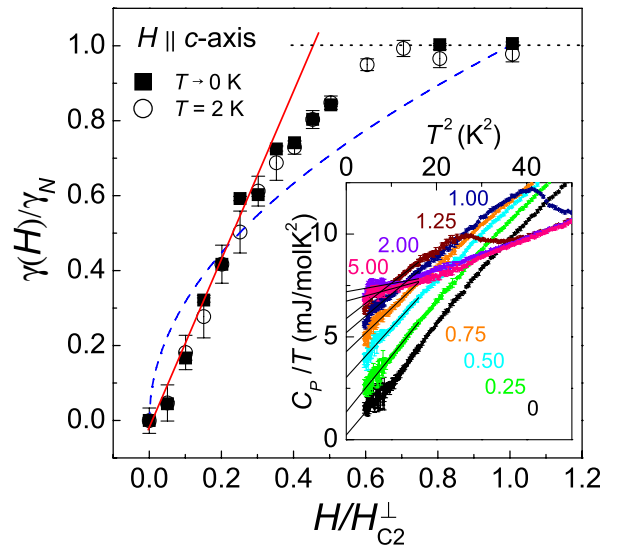


FIG. 4 (color online). Magnetic field dependence of  $\gamma(H)$  as a function of  $H/H_{c2}^\perp$ .  $\gamma(H)$  for  $T \rightarrow 0$  K (■) and at  $T = 2$  K (○) is normalized by  $\gamma_N = \gamma(10 \text{ kOe})$ . The (red) solid and (blue) dashed lines correspond to  $\gamma(H) \propto H$  and  $\gamma(H) \propto H^{1/2}$ , respectively. The (black) dotted line indicates  $\gamma(H)/\gamma_N = 1$ . Inset: Low temperature  $C_P$  data at various magnetic fields. The (black) solid lines are fits to the data for  $2 \text{ K} \leq T \leq 4 \text{ K}$ . The numbers next to the data correspond to the magnetic fields (kOe).

adverse to  $\gamma(H) \propto H^{1/2}$  expected for nodal superconductivity and also in contrast to two-band superconductivity [20]. Recent calculations found that even for an isotropic-gapped type-II superconductor,  $\gamma(B) \propto B$  behavior persists only up to a certain crossover field,  $B^*$  [21]. For the isotropic superconducting gap,  $B^*$  is expected to be  $\approx 0.32B_{c2}$ , which is reduced as the degree of the anisotropy for the superconducting gap increases. Since  $C_p(H)$  measurements were done in the field-cooled mode, we can approximately estimate the ratio between the crossover field and the upper critical field  $B^*/B_{c2} \approx H^*/H_{c2} \sim 0.3$ , which is quite close to the isotropic limit. Thus the magnetic field dependence of  $\gamma(H)$  consistently supports the notion of a fully gapped and almost isotropic superconducting order parameter [22].

Finally, we estimate the  $e$ -ph coupling strength  $\lambda$  for  $\text{CaC}_6$ . From a comparison between  $\gamma_N$  and the density of states at the Fermi level  $E_F$ ,  $N(0)$ ,  $\lambda$  can be estimated using the equation  $\gamma_N = (2\pi^2 k_B^2/3)N(0)(1 + \lambda)$ . If we take  $N(0) = 1.50$  states/eV · cell from recent calculations [9], we obtain  $\lambda = 0.70 \pm 0.04$  with our  $\gamma_N = 6.01 \pm 0.14$  mJ/mol K<sup>2</sup>.  $T_c$  is estimated from the experimentally determined  $\lambda$  and  $\Theta_D$  using the McMillan formula [23],

$$T_c = \frac{\Theta_D}{1.45} \exp\left[\frac{-1.04(1 + \lambda)}{\lambda - (1 + 0.62\lambda)\mu^*}\right], \quad (1)$$

where  $\mu^*$  is Coulomb pseudopotential. Taking  $\mu^* = 0.15$ , we obtain  $T_c = 11 \text{ K} \pm 2 \text{ K}$ , which is in good agreement with the measured  $T_c$ . This implies that the relatively high  $T_c$  in  $\text{CaC}_6$  can be understood in terms of the intermediate  $e$ -ph coupling. Recent calculations [9] predicted  $\lambda$  to be  $\approx 0.83$ , in reasonable agreement with the measured  $\lambda$ .

In conclusion, we have reported the first specific heat measurements for the superconducting and normal state of high-quality bulk  $\text{CaC}_6$  samples. The specific heat anomaly at  $T_c$  is clearly resolved indicating the bulk nature of the superconductivity. Both the temperature and magnetic field dependence of  $C_p$  strongly suggests a fully gapped superconducting order parameter. Very recently, Lamura *et al.* [24] reported an exponential temperature dependence of the in-plane penetration depth for  $\text{CaC}_6$  indicating a fully gapped superconductivity, which is consistent with our  $C_p$  study. The estimated  $e$ -ph coupling constant  $\lambda$  from the specific heat measurements is  $0.70 \pm 0.04$ , in reasonable agreement with recent calculations [9]. These results suggest that  $\text{CaC}_6$  is a fully gapped, intermediate-coupled, phonon-mediated superconductor without essential contributions from alternative pairing mechanisms. Together with alkali-metal intercalated fullerenes and  $B$ -doped diamond,  $\text{CaC}_6$  is another  $e$ -ph coupled superconductor, which demonstrates the richness of the  $e$ -ph pairing routes in carbon-based superconducting systems.

We acknowledge D. Guerard and A. Simon for sharing ideas about intercalation chemistry. We thank E. Brucher,

G. Siegle, and C. Hoch for experimental support, and W. Schnelle, B. Mitrović, O. V. Dolgov, and O. K. Andersen for discussions.

\*Electronic address: js.kim@fkf.mpg.de

- [1] T. E. Weller, M. Ellerby, S. S. Saxena, R. P. Smith, and N. T. Skipper, *Nature Phys.* **1**, 39 (2005).
- [2] N. Emery *et al.*, *Phys. Rev. Lett.* **95**, 087003 (2005).
- [3] For a review, see M. S. Dresselhaus and G. Dresselhaus, *Adv. Phys.* **51**, 1 (2002).
- [4] G. Csányi, P. B. Littlewood, A. H. Nevidomskyy, C. J. Pickard, and B. D. Simons, *Nature Phys.* **1**, 42 (2005).
- [5] W. A. Little, *Phys. Rev.* **134**, A1416 (1964); Y. A. Uspenski and G. F. Zharkov, *Zh. Eksp. Teor. Fiz.* **65**, 1460 (1973) [*JETP* **34**, 1132 (1972)]; D. Allender, J. Bray, and J. Bardeen, *Phys. Rev. B* **7**, 1020 (1973).
- [6] A. Bill, H. Morawitz, and V. Z. Kresin, *Phys. Rev. B* **68**, 144519 (2003).
- [7] S. Yamanaka, K. Hotehama, and H. Kawaji, *Nature (London)* **392**, 580 (1998).
- [8] I. I. Mazin, *Phys. Rev. Lett.* **95**, 227001 (2005).
- [9] M. Calandra and F. Mauri, *Phys. Rev. Lett.* **95**, 237002 (2005).
- [10] The intensity ratio of the reflections from the impurity phase and the  $\text{CaC}_6$  phase is  $< 1\%$ .
- [11] S. Pruvost, C. Hérol, A. Hérol, and P. Lagrange, *Eur. J. Inorg. Chem.* **2004**, 1661 (2004).
- [12] U. Mizutani, T. Kondow, and T. B. Massalski, *Phys. Rev. B* **17**, 3165 (1978).
- [13] J. S. Kim, L. Boeri, R. K. Kremer, and F. S. Razavi, *cond-mat/0603530*.
- [14] P. Delhaes, J. C. Rouillon, J. P. Manceau, D. Guerard, and A. Herold, *J. Phys. Lett.* **37**, 127 (1976); C. Ayache, E. Bonjour, R. Lagnier, and J. E. Fischer, *Physica (Amsterdam)* **99B**, 547 (1980).
- [15] H. Padamsee, J. E. Neighbor, and C. A. Shiffman, *J. Low Temp. Phys.* **12**, 387 (1973).
- [16] F. Bouquet *et al.*, *Europhys. Lett.* **56**, 856 (2001); A. A. Golubov *et al.*, *J. Phys. Condens. Matter* **14**, 1353 (2002).
- [17] N. R. Werthammer, E. Helfand, and P. C. Hohenberg, *Phys. Rev.* **147**, 295 (1966).
- [18] Y. Koike, H. Suematsu, K. Higuchi, and S. Tanuma, *Physica (Amsterdam)* **99B**, 503 (1980); A. Chaiken *et al.*, *Phys. Rev. B* **41**, 71 (1990).
- [19] G. E. Volovik, *JETP Lett.* **58**, 469 (1993).
- [20] F. Bouquet, R. A. Fisher, N. E. Phillips, D. G. Hinks, and J. D. Jorgensen, *Phys. Rev. Lett.* **87**, 047001 (2001); H. D. Yang *et al.*, *ibid.* **87**, 167003 (2001).
- [21] N. Nakai, P. Miranović, M. Ichioka, and K. Machida, *Phys. Rev. B* **70**, 100503(R) (2004).
- [22] The possible anisotropic or multigap nature might be smeared out due to a certain level of disorder in the system, e.g., the intercalated Ca distribution. However, the difference, if any, between the largest and smallest gaps will be rather small.
- [23] W. L. McMillan, *Phys. Rev.* **167**, 331 (1968).
- [24] G. Lamura *et al.*, *Phys. Rev. Lett.* **96**, 107008 (2006).